Changes in Retinal Nerve Fiber Layer Reflectance Intensity as a Predictor of Functional Progression in Glaucoma

Stuart K. Gardiner, Shaban Demirel, Juan Reynaud, and Brad Fortune

Devers Eye Institute, Legacy Health, Portland, Oregon, United States

Correspondence: Stuart K. Gardiner, Devers Eye Institute, Legacy Health, 1225 NE 2nd Avenue, Portland, OR 97232, USA; sgardiner@deverseye.org.

Submitted: December 3, 2015
Accepted: February 13, 2016

Citation: Gardiner SK, Demirel S, Reynaud J, Fortune B. Changes in retinal nerve fiber layer reflectance intensity as a predictor of functional progression in glaucoma. *Invest Ophthalmol Vis Sci.* 2016;57:1221–1227. DOI:10.1167/iovs.15-18788

Purpose. We determined whether longitudinal changes in retinal nerve fiber layer (RNFL) reflectance provide useful prognostic information about longitudinal changes in function in glaucoma.

Methods. The reflectance intensity of each pixel within spectral-domain optical coherence tomography (SD-OCT) circle scans was extracted by custom software. A repeatability cohort comprising 53 eyes of 27 participants (average visual field mean deviation [MD] −1.65 dB) was tested five times within a few weeks. To minimize test–retest variability in their data, a reflectance intensity ratio was defined as the mean reflectance intensity of pixels within the RNFL divided by the mean between the RNFL and RPE. This was measured in a separate longitudinal cohort comprising 310 eyes of 205 participants tested eight times at 6-month intervals (average MD, −0.99 dB; median rate of change, −0.09 dB/y). The rate of change of this ratio, together with the rate of RNFL thinning, and their interaction, were used to predict the rate of change of MD.

Results. In univariate analyses, the rate of RNFL thinning was predictive of the rate of MD change ($P < 0.0001$), but the rate of change of reflectance intensity ratio was not ($P = 0.116$). However, in a multivariable model, the interaction between these two rates significantly improved upon predictions of the rate of functional change made using RNFL thickness alone ($P = 0.038$).

Conclusions. For a given rate of RNFL thinning, a reduction in the RNFL reflectance intensity ratio is associated with more rapid functional deterioration. Incorporating SD-OCT reflectance information may improve the structure–function relation in glaucoma.

Keywords: OCT, RNFL, reflectance

Spectral-domain optical coherence tomography (SD-OCT) allows three-dimensional visualization and measurement of ocular structures with high resolution. To date, most parameters derived from SD-OCT scans for clinical application relate to the anatomical dimensions of a particular structure. Tools have been developed to measure automatically the thickness of the retinal nerve fiber layer (RNFLT), ganglion cell complex, and/or other individual retinal layers, as well as optic nerve head parameters, such as neuroretinal minimum rim width and area, among others. However, more information may be available than just the dimensions of these structures. For example, image contrast based on detection of motion forms the basis for various approaches to OCT angiography.[1,2] Polarization-sensitive OCT exploits variation between tissue layers of the intrinsic optical property birefringence to enhance boundary contrast and to reveal information about ultrastructure within a given tissue layer.[3,4] Other approaches, such as optophysiology, seek to detect activity-dependent changes in retinal reflectivity.[5] In the current study, we tested the hypothesis that intrinsic optical properties of tissues may have prognostic value for glaucoma, when assessed using surrogate measurements, such as reflectance intensity, that can be extracted from conventional SD-OCT scans.

It is well known that the reflectance of the retinal nerve fiber layer (RNFL) bundles is highly directional and spectrally dependent.[6–8] Loss of axons from the RNFL, especially when loss is concentrated within specific axon bundles, leads to the appearance of RNFL bundle defects, thought to be one of the earliest clinical signs of glaucoma.[9,10] However, it also is known that RNFL reflectance depends on the integrity of the axonal cytoskeletal ultrastructure.[11,12] Consequently, it has been hypothesized that disruption of the axonal cytoskeleton after glaucomatous or other injury might manifest as altered RNFL reflectance, and that these alterations could potentially occur before axons undergo complete and irreversible degeneration.[13] It has been reported that relative internal reflectivity, defined as the mean reflectivity of pixels within the RNFL divided by the saturation reflectivity, was reduced in eyes with glaucoma and was correlated to RNFL thickness.[14] In addition, a reduction in the reflectance of nerve fiber bundles before RNFL thinning has been reported in a rat model of glaucoma, using a multispectral imaging microreflectometer to evaluate retinal explant preparations.[11]

It also has been reported that decreased RNFL reflectance was correlated with increased IOP in a sample of three eyes from a nonhuman primate model of glaucoma,[15] with "reflectance" in this case measured by SD-OCT and defined as the ratio of the intensity of the RNFL to the intensity of a thin layer around the RPE. This normalized reflectance, also referred to as an RPE-referenced attenuation coefficient, has been applied to human SD-OCT scans,[16] and shown to distinguish well between glaucomatous eyes and normal controls.[17]

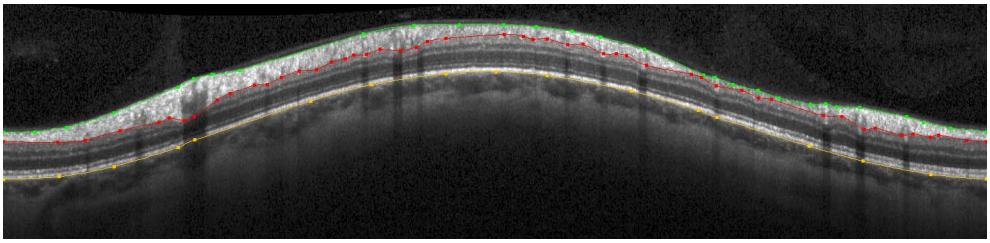

FIGURE 1. Example of a circle scan of the peripapillary RNFL. Three structures are delineated: the ILM (*green*), posterior border of the RNFL (*red*), and the posterior border of the RPE (*yellow*). The scan is presented (*left* to *right*) as temporal – superior – nasal – inferior – temporal.

In this study, we ask whether observable changes in the average reflectance of the RNFL over time correspond to progressive functional changes. These changes could be caused by axonal dysfunction and/or by a time lag between axonal death and consequent RNFL thinning. We define an "intensity ratio," similar to the normalized reflectance index,[17] but using a wider reference area for the normalization step. Instead of using physiologic models of the propagation of light in tissue to derive a theoretically-optimal measure of reflectance,[16] we use numerical methods in an attempt to choose a measure that can be obtained with lower variability. We then examine whether longitudinal changes in this intensity ratio are associated with changes in perimetric sensitivity in human glaucoma. If changes in reflectance over time are associated with more rapid functional deterioration within that same time period, then this would support the hypothesis that it is a characteristic part of the glaucomatous disease process and a potentially useful biomarker for clinical application.

METHODS

Population

Data for this study were obtained from participants in the Portland Progression Project, a prospective longitudinal study of the course and risk factors for glaucomatous progression. Individuals with non-end-stage glaucoma or with ocular hypertension plus risk factors for glaucoma undergo testing with a variety of methods, including automated perimetry and SD-OCT. Two separate cohorts were used: a "repeatability cohort," consisting of participants tested five times within a few months, and a "longitudinal cohort," consisting of participants tested approximately every 6 months over several years. Longitudinal data were used from the most recent eight visits at which reliable measurements (as outlined below) were acquired.

Participants were tested at Devers Eye Institute (Portland, OR, USA). Inclusion criteria for both cohorts were a diagnosis of primary open-angle glaucoma and/or likelihood of developing glaucomatous damage (e.g., high-risk ocular hypertension), as determined at the discretion of each participant's physician. A visual field defect was not a requirement for study entry. Exclusion criteria at entry included an inability to perform reliable visual field testing, best-corrected visual acuity worse than 20/40, or other conditions or medications that may affect the visual field. All protocols were approved and monitored by the Legacy Health Institutional Review Board, and adhered to the Health Insurance Portability and Accountability Act of 1996 and the tenets of the Declaration of Helsinki. All participants provided written informed consent once all of the risks and benefits of participation were explained to them.

Testing Protocol

Functional testing was performed using automated white-on-white perimetry with a Humphrey Field Analyzer (HFA II; Carl-Zeiss Meditec, Dublin, CA, USA), with a size III stimulus, SITA standard algorithm, and 24-2 test pattern. Visual field tests were excluded from analysis if they had greater than 33% false-negatives, 20% false-positives, or 33% fixation losses. For the primary analysis, mean deviation (MD) was used, representing the global status of the visual field relative to age-appropriate normals, summarized across the 52 locations (excluding the blind spot) in the field. Since it has been reported that the structure–function relation may be nonlinear,[18,19] and that functional progression also may be nonlinear when expressed in decibels,[20,21] a second summary functional measure was calculated. The linear mean sensitivity (LMS) was defined as the arithmetic mean of pointwise sensitivities expressed on a linear scale of $10^{(dB - 30)/10}$, so that 0 dB → 0.001, 10 dB → 0.01, 20 dB → 0.1, and 30 dB → 1.0. Sensitivities on this scale then may be more linearly related to axon counts and, hence, to RNFLT,[18,19] and also may progress more linearly over time.[20,21]

Spectral-domain OCT was performed with a Spectralis OCT (Heidelberg Engineering, Heidelberg, Germany). On each test date, a circle scan was performed at a radius of 6° from the center of the optic disc as placed by the operator. Images were focused by the technician aiming to optimize the clarity of blood vessels within the RNFL. Follow-up scans were registered in real-time to the location of the baseline reference scan for each eye. Three segmentations were delineated on each circular B-scan, as shown in the example in Figure 1; the inner limiting membrane (ILM, in green), the posterior border of the RNFL (in red), and the posterior border of the RPE/Bruch's membrane (in yellow). The instrument's automated delineations were adjusted manually by experienced technicians when necessary to address obvious delineation errors (without reference to the functional results). The pixel corresponding to each of these three boundaries was recorded for each A-scan. In each case, this boundary pixel was assigned as belonging to the layer below the boundary; hence pixels along the red line in Figure 1 are counted not as part of the RNFL, but as part of the retinal ganglion cell layer. Peripapillary RNFLT was defined as the mean distance between the green and red lines.

Measurement of Reflectance Intensity

For each pixel within the circle scan, the intensity of the raw reflectance image was extracted using custom software. Since overall tissue reflectance varies between scans and between individuals, due to factors including differences in the exact focal plane and the quality of preretinal optics, normalization is required to better represent alterations of the tissues' inherent optical properties rather than the influence of these imaging

Investigative Ophthalmology & Visual Science

Table 1. Summary of the Characteristics of the Two Cohorts

	Mean	SD	Range
Repeatability cohort			
Series length, d	39.2	10.6	27 to 69
Age, y	65.1	9.5	50 to 94
MD, dB	−1.65	4.25	−23.3 to +2.3
RNFLT, μm	81.5	16.0	34 to 109
Longitudinal cohort			
Series length, y	4.7	0.5	3.5 to 5.5
Age at end of series, y	69.5	9.8	41 to 90
Most recent MD, dB	−0.99	3.07	−20.42 to +2.97
Rate of change of MD, dB/y	−0.13	0.34	−2.8 to +0.5
Most recent RNFLT, μm	84.7	15.7	33 to 123
Rate of change of RNFLT, μm/y	−0.75	1.32	−11.9 to +3.8

Rates of change were calculated by linear regression over the 8 most recent reliable tests for an eye. Only eyes with at least 8 reliable tests were included in the longitudinal cohort.

Table 2. Summary of the Per-Eye Coefficients of Variation (i.e., SD Divided by Mean) of Reflectance Intensity Ratio, Using Five Different Normalization Methods

Region Used for Normalization	Mean	SD	Range
Posterior vitreous	23.5%	11.1%	4.3%–49.1%
Pixels coinciding with posterior border of RPE	19.5%	8.4%	5.6%–40.7%
5-pixel wide band above posterior border of RPE	18.8%	8.9%	5.3%–40.3%
11-pixel wide band centered on posterior border of RPE	19.0%	8.7%	6.2%–39.5%
All pixels between posterior borders of RPE and RNFL	16.8%	7.8%	5.0%–37.0%

Data were taken from 53 eyes of 27 participants in the repeatability cohort, scanned five times each over a period of a few weeks. Each intensity ratio is defined as the mean intensity of pixels within the RNFL divided by the mean intensity of pixels within the listed area, as defined in the Methods section.

artefacts. Five methods for normalizing the reflectance intensity values were considered: (1) the mean intensity of pixels within the RNFL divided by the mean intensity of pixels within the posterior vitreous (i.e., above the ILM), (2) the mean intensity of pixels within the RNFL divided by the mean intensity of pixels coinciding with the delineated posterior border of the RPE (the yellow line on Fig. 1), (3) the mean intensity of pixels within the RNFL divided by the mean intensity of a 5-pixel wide band immediately above the delineated posterior border of the RPE (designed to be entirely within the high reflectance region of RPE visible on Fig. 1), (4) the mean intensity of pixels within the RNFL divided by the mean intensity of an 11-pixel wide band centered on the delineated posterior border of the RPE (designed to be similar to the method used by Dwelle et al.[15]), and (5) the mean intensity of pixels within the RNFL divided by the mean intensity of sub-RNFL tissue, extending from one pixel below the posterior border of the RNFL to the posterior border of the RPE (i.e., between the red and yellow lines in Fig. 1; chosen under the assumption that using a larger portion of the cross-sectional B-scan image should provide increased stability and, hence, lower variability, especially in the face of variability caused by the precise delineation of the retinal layers).

Using each of these normalizations in turn, an intensity ratio was calculated for each scan in the repeatability cohort. The standard deviation of the five values for the scans obtained from each eye was calculated, and expressed as a percentage of the mean value. Therefore, there is one coefficient of variation per eye. This coefficient of variation can be considered equivalent to the reciprocal of the signal-to-noise ratio, under the assumption that the mean value is representative of the magnitude of the signal. To determine the most repeatable measure of reflectance intensity, these were compared between normalization techniques using the signed rank test for clustered data developed by Datta and Satten,[22,23] since data from both eyes were used. The least variable measure then was selected for application in the longitudinal cohort.

Prediction of Functional Change

The per-eye rate of change over the most recent 8 visits in the longitudinal cohort was calculated by least-squares linear regression, for the two structural measures RNFLT and reflectance intensity ratio, and for the two functional measures MD and LMS. Models then were formed to predict the rate of functional change (by MD or LMS), using the concurrent rate of change of RNFLT, the rate of change of the reflectance intensity ratio, and their interaction. Since rates of change from both eyes were calculated, a generalized estimating equation (GEE) model was used to account for correlation between the two eyes of an individual. To assess whether disease severity affected the results, secondary analyses were performed after splitting the data into two halves, according to whether the final MD in the visual field series for an eye was greater or less than the median value. Analyses were performed using the R language and environment for statistical computing (Version 2.15.3; R Core Team, Vienna, 2013, available in the public domain at http://www.R-project.org/).

Results

Population

The repeatability cohort consisted of 53 eyes of 27 participants (one eye was excluded due to an ocular pathology unrelated to glaucoma), tested 5 times per eye within a relatively short period of time. The longitudinal cohort (restricted to eyes with at least 8 visits at which data of sufficient quality were obtained for SD-OCT and perimetry) consisted of 310 eyes of 205 participants. Characteristics of the two cohorts are summarized in Table 1. The median rate of change of MD (from linear regression) in the longitudinal cohort was –0.09 dB/y, similar to a report from a clinical population of patients with glaucoma.[24]

Measurement of Reflectance Intensity

Table 2 summarizes the per-eye coefficients of variation within the repeatability cohort for each of the five normalization techniques considered. Using the entire region from the posterior border of the RNFL down to the posterior border of the RPE (i.e., between the red and yellow lines on Fig. 1, Method 5 in the list above) had significantly lower coefficients of variation (using the signed-rank test for clustered data[22]) than normalizations based on the posterior vitreous ($P = 0.011$) or any of the three methods that relied upon RPE-based normalization (all $P < 0.001$). Therefore, Method 5 was used to define the reflectance intensity ratio when analyzing data from the longitudinal cohort. The 95% confidence interval for test–retest using this method was ±33% of the value. The effect of the chosen normalization on intertest variability in the repeatability cohort is illustrated in Figure 2. Note that for comparison, RNFLT had an average coefficient of variation in this cohort of just 1.3% (range, 0.3%–4.5%).

Investigative Ophthalmology & Visual Science

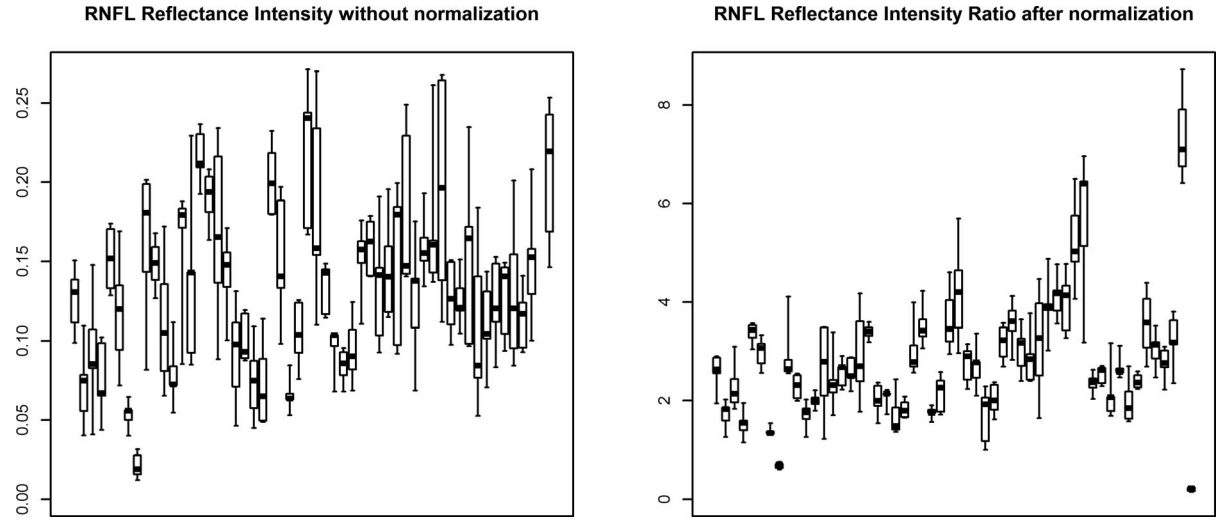

FIGURE 2. The effect of normalization on reflectance intensity measures in the repeatability cohort. For each eye, the median of the five measured values is marked by a *black square*. The *box* extends from the second lowest to the second highest measurements; the *whiskers* extend to the minimum and maximum measurements for that eye. After normalization, the within-eye variability (shown by *width* of each *box*) is reduced as a proportion of the between-eye variability. Therefore, it can be seen that normalization based on the average reflectance of pixels between the nerve fiber layer and RPE greatly improves test–retest variability in this cohort, for which no true change should have occurred.

Prediction of Functional Change

The mean of the chosen reflectance intensity ratio across all eyes and all visits in the longitudinal cohort was 2.69 (SD, 0.99; range, 1.01–7.28). The mean per-eye rate of change of the reflectance intensity ratio in this cohort was –0.06 y^{-1} (SD, 0.22 y^{-1}; range, –0.90 to +1.13 y^{-1}). The rate for a given eye was used together with the rate of change of RNFLT to predict the rate of functional change.

In univariate analyses, the rate of RNFL thinning was predictive of the rate of MD change, with $P < 0.0001$; *d/dt* MD = –0.062 + 0.096 × *d/dt* RNFLT (where *d/dt X* represents the rate of change of measure *X* over time). The value of *d/dt* MD is measured in dB/y, and *d/dt* RNFLT is measured in μm/y. The rate of change of the reflectance intensity ratio was not by itself significantly predictive of the rate of MD change ($P = 0.116$). However, in a multivariable model, the interaction between the two structural rates of change improved upon predictions of the rate of functional change made using the rate of RNFLT change alone:

$$\frac{d}{dt}MD = -0.065 + \left(0.079 \times \frac{d}{dt}RNFLT\right) - \left(0.101 \times \frac{d}{dt}RNFLT \times \frac{d}{dt}Reflectance\ Intensity\ Ratio\right).$$

In this model, *d/dt* RNFLT had $P = 0.0005$ and the interaction term had $P = 0.038$.

As an example of the effect size: the average value of *d/dt* RNFLT from the longitudinal cohort was –0.75 μm/y. For this rate of RNFL thinning, if the reflectance intensity ratio changed at +1.13 y^{-1} (the highest value observed), then the predicted rate of functional change would be *d/dt* MD = –0.04 dB/y. By contrast, if the reflectance intensity ratio changed at –0.90 y^{-1} (the lowest value observed) then the predicted rate would be *d/dt* MD = –0.19 dB/y, representing nearly a five times more rapid rate of functional deterioration.

When sensitivities were transformed from dB to a linear scale, results generally were similar. *d/dt* RNFLT was predictive of *d/dt* LMS, with $P = 0.0001$, but the rate of change of reflectance intensity ratio was not significantly predictive, with $P = 0.256$. However, in the multivariable model,

$$\frac{d}{dt}LMS = -0.0214 + \left(0.0081 \times \frac{d}{dt}RNFLT\right) - \left(0.0178 \times \frac{d}{dt}RNFLT \times \frac{d}{dt}Reflectance\ Intensity\ Ratio\right)$$

where *d/dt RNFLT* had $P = 0.002$ and the interaction term had $P = 0.009$.

Secondary analyses were performed after splitting the cohort into two equal parts based on the final MD in each eye's series. Among those eyes with final MD worse than –0.15 dB (the median value in the cohort), in the same multivariable model as before, *d/dt RNFLT* still was a significant predictor of *d/dt MD* with $P = 0.0024$, but the interaction term had $P = 0.650$. By contrast, among eyes with final MD greater than –0.15 dB, *d/dt RNFLT* had $P = 0.1092$, while the interaction term had $P = 0.0653$. Clearly these results are not definitive, since they did not reach statistical significance (possibly due to the reduced sample size), but they hint that changes in reflectance intensity may be most useful at the earliest stages of the disease process.

DISCUSSION

Retinal nerve fiber layer thickness remains an excellent structural measure for use in the diagnosis and monitoring of glaucoma.[25–27] It is highly repeatable; the average per-eye coefficient of variation in our repeatability cohort was 1.3%, which is similar to the 1.9% intravisit coefficient of variation reported previously for the Cirrus OCT (Carl-Zeiss Meditec, Inc.).[28] In our longitudinal cohort, the cross-sectional correlation between RNFLT and MD was 0.613. Longitudinally, by contrast, the correlation between the rates of change of RNFLT and MD was only 0.361. In part, this is because the range of values is narrower, and so the value of the correlation coefficient is reduced. However, it also suggests that other sources of information are needed to refine predictions of longitudinal functional change. As shown here, the reflectance of the RNFL appears to provide one such source. It is possible that reflectance will prove to be even more useful in eyes with

Investigative Ophthalmology & Visual Science

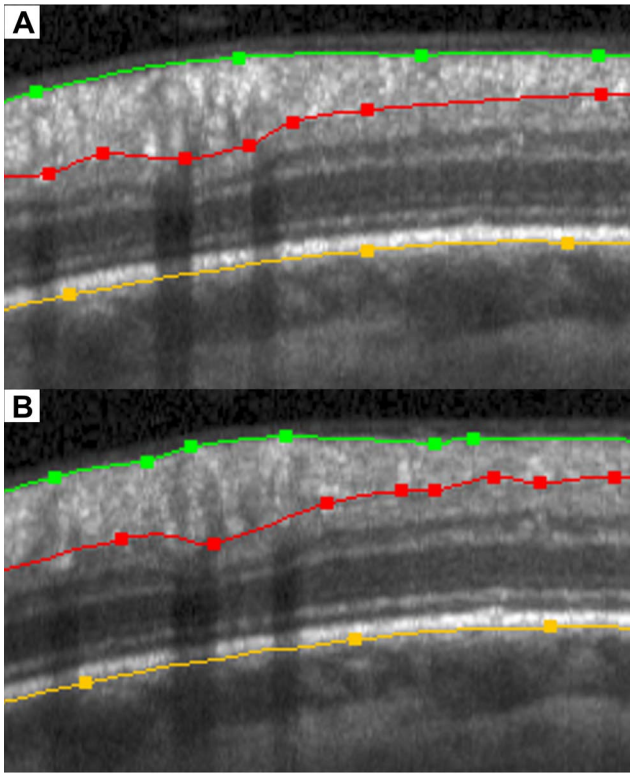

FIGURE 3. Example of a section of an OCT scan (*top*), and the same section 18 months later (*bottom*). In that time period, the nerve fiber layer has not thinned, but the reflectance intensity has decreased. This corresponded to worsening function during that same period.

very early damage and/or ocular hypertension. Importantly, reflectance information can be extracted from existing SD-OCT scans without hardware modifications.

It is important to note that the reflectance intensity ratio by itself was not predictive of functional change. It is not a replacement for using RNFLT. Instead, it provides a method that may be able to refine predictions made using RNFLT. Longitudinal changes observed in the reflectance must be considered in the context of changes observed in the RNFLT, and not interpreted in isolation.

It certainly is possible that the measure of reflectance intensity used here might be improved upon. Most commercial OCT instruments are optimized to visualize cross-sectional (B-scan) images and to measure the thickness of structures in the retina, not their reflectance. Consequently, it may be possible to improve the intensity data obtained. For example, improvements could involve removing the effects of vessel shadows, and/or taking into account the directionality of retinal reflectance.[7,8,29] Directionality is particularly important for cylindrical structures, such as axons and their aligned cytoskeletal components,[7] which our normalization procedures, therefore, do not address. Indeed, the test–retest variability of our measure shown in Figure 2 still is more than 10 times higher than the variability of RNFLT measurement. Improvements in the repeatability of the reflectance intensity ratio would likely improve its use for prediction of functional change. In this study, the interaction between reflectance and thickness improved prediction of the rate of MD change, but this was only just significant with $P = 0.038$. Accordingly, the standard deviation of residuals (i.e., predicted rate minus observed rate) was reduced by less than 5% by the inclusion of reflectance intensity ratio. If the test–retest variability of reflectance intensity could be improved further, then we would anticipate this P value being reduced. Moreover, commercial instruments may apply automatic gain controls to maintain signal strength in a more ideal range, providing benefits to imaging a broader range of eyes, but potentially confounding reflectance intensity measurements (especially those without some internal normalization).

We also would note that it is possible that reflectance intensity may change before or after RNFL thinning. This study did not incorporate any potential time lag between the observed changes in the retina, since each measure was assumed to change linearly over time. Furthermore, we looked solely at concurrent rates of functional change; the aim was to predict the rate of functional loss during that same time period, rather than to predict subsequent functional loss.

Previous studies have used a narrow band around the RPE to normalize RNFL reflectance,[15,17] but used multiple B-scans at different radial distances from the center of the optic nerve head. By contrast, in this study a single circle scan at 6° from the center of the optic nerve head was used. This is consistent with the most common current clinical approach, but means fewer pixels of information are available (1536 for this analysis) and a more limited area of RNFL is assayed by the single circular scan. Using a thicker band of axial information extending all the way from the posterior border of the RNFL down to the RPE increased the number of available pixels, and so appears to give a more reliable measure of sub-RNFL reflectance when a single circle scan is used. Correspondingly, the test–retest variability of the reflectance intensity ratio was lower when using this thicker band. It should be noted, though, that while we tested several alternative methods for interscan normalization, these do not represent an exhaustive examination of all possibilities, and further improvement may be possible.

The data used in this study consist primarily of cases of early, well-managed glaucoma. Only 4 of the 53 eyes in the repeatability cohort, and 20 of 310 eyes in the longitudinal cohort, had MD worse than –6 dB, a value often taken to indicate moderate functional damage. Approximately half of the eyes did not yet have significant functional damage when assessed by MD alone. Therefore, this represents an extremely important clinical scenario, where early signs of functional progression are sought. Indeed, the secondary analyses hint that reflectance intensity may be more useful in "preperimetric glaucoma" than in eyes with established functional defects, although we cannot conclude this definitively at the present time. However, our conclusions have not been tested in cases of more severe glaucoma, and so it is not yet known whether reflectance intensity remains a useful prognostic measure later in the disease process or whether it represents a very early stage of structural damage. We also would note that this study aims to predict the rate of change of MD, because we sought a single continuous variable as the outcome measure to increase the statistical power of the analysis; yet this is known not to be a particularly sensitive measure of visual field change,[30] especially early in the disease process. Future studies are needed that examine pointwise progression, and/or with much larger cohorts that would enable assessment using binary definitions of progression and stability.

This study should be considered a "proof of principle," rather than providing a measurement that is ready to be implemented into commercially-available instruments, given the high test–retest variability of the reflectance intensity ratio used here. However, the principle behind the measurement is something that can be qualitatively assessed already, even if quantitative assessment is not yet clinically available. Figure 3 shows a magnified portion (for easier visualization) of the

peripapillary RNFL B-scan shown in Figure 1; together with the corresponding portion of a scan from the same eye 18 months later. On the date of the first (upper) scan, this participant had an average RNFLT of 91.2 μm and a reflectance intensity ratio averaged around the entire circle scan of 4.73. Using the variability estimate from Table 2, this means that the 95% confidence interval for test–retest is (3.17, 6.29). By the date of the second (lower) scan, the RNFLT essentially was unchanged at 92.3 μm. However, the reflectance intensity ratio had decreased to 2.87. The nerve fiber layer is visibly less reflective in the lower panel. Within the same time period, the MD decreased from −5.0 dB on the date of the first scan to −7.6 dB on the date of the second scan. The results of this study suggested that clinicians should be on the lookout for similar decreases in RNFL reflectance, as they may correspond (as in this example) to worsening function.

In practice, light intensity and focus may vary between scans, with the result that changes in reflectance will not always be easily visible to the clinician. Furthermore, to map the raw intensity information to a range compatible with most common monitors and/or clinical printouts, raw intensity values are compressed to 256 grayscale levels (8-bit range), reducing the precision available. Our normalization process (which is applied to raw intensity data) may not be easy to implement qualitatively while reviewing a series of scans in a clinical setting. Therefore, it is hoped that instrument manufacturers could eventually add such measures to their output, enabling more sensitive detection of changes in reflectance.

In summary, we described a method to quantify the reflectance intensity of the RNFL from SD-OCT scans. For a given rate of RNFL thinning, a reduction in RNFL reflectance is associated with more rapidly deteriorating function. Further work will examine whether localized changes in RNFL reflectance correspond to localized functional deterioration. The causes of these reductions in reflectance intensity are not entirely clear, but they raise the intriguing possibility of dysfunctional yet surviving ganglion cell axons, which may be candidates for neuroprotection or rescue. Clinically, we would recommend examination of the images produced by OCT instruments, as they may reveal important changes that are not apparent from looking at RNFL thickness or other structural measures in isolation.

Acknowledgments

Presented in part at the annual meeting of the Association for Research in Vision and Ophthalmology (ARVO), Denver, Colorado, United States, May 3–7, 2015.

Supported by National Institutes of Health (NIH: Bethesda, MD, USA) Grants NIH R01-EY020922 (SKG), NIH R01-EY019674 (SD), and NIH R01-EY019327 (BF); and unrestricted research support from The Legacy Good Samaritan Foundation (Portland, OR, USA). The authors alone are responsible for the content and writing of this paper.

Disclosure: **S.K Gardiner**, None; **S. Demirel**, None; **J. Reynaud**, None; **B. Fortune**, None

References

1. Jia Y, Morrison JC, Tokayer J, et al. Quantitative OCT angiography of optic nerve head blood flow. *Biomed Opt Express*. 2012;3:3127–3137.
2. Jia Y, Wei E, Wang X, et al. Optical coherence tomography angiography of optic disc perfusion in glaucoma. *Ophthalmology*. 2014;121:1322–1332.
3. Pircher M, Hitzenberger CK, Schmidt-Erfurth U. Polarization sensitive optical coherence tomography in the human eye. *Prog Retin Eye Res*. 2011;30:431–451.
4. Cense B, Chen TC, Park BH, Pierce MC, de Boer JF. In vivo depth-resolved birefringence measurements of the human retinal nerve fiber layer by polarization-sensitive optical coherence tomography. *Optics Lett*. 2002;27:1610–1612.
5. Bizheva K, Pflug R, Hermann B, et al. Optophysiology: depth-resolved probing of retinal physiology with functional ultrahigh-resolution optical coherence tomography. *Proc Natl Acad Sci U S A*. 2006;103:5066–5071.
6. Knighton RW, Jacobson SG, Kemp CM. The spectral reflectance of the nerve fiber layer of the macaque retina. *Invest Ophthalmol Vis Sci*. 1989;30:2392–2402.
7. Knighton RW, Huang XR. Directional and spectral reflectance of the rat retinal nerve fiber layer. *Invest Ophthalmol Vis Sci*. 1999;40:639–647.
8. Huang X-R, Knighton RW, Feuer WJ, Qiao J. Retinal nerve fiber layer reflectometry must consider directional reflectance. *Biomed Opt Express*. 2016;7:22–33.
9. Hoyt WF, Newman NM. The earliest observable defect in glaucoma? *Lancet*. 1972;1:692–693.
10. Hoyt WF, Frisen L, Newman NM. Fundoscopy of nerve fiber layer defects in glaucoma. *Invest Ophthalmol*. 1973;12:814–829.
11. Huang X-R, Zhou Y, Kong W, Knighton RW. Reflectance decreases before thickness changes in the retinal nerve fiber layer in glaucomatous retinas. *Invest Ophthalmol Vis Sci*. 2011;52:6737–6742.
12. Huang XR, Knighton RW, Cavuoto LN. Microtubule contribution to the reflectance of the retinal nerve fiber layer. *Invest Ophthalmol Vis Sci*. 2006;47:5363–5367.
13. Huang XR, Bagga H, Greenfield DS, Knighton RW. Variation of peripapillary retinal nerve fiber layer birefringence in normal human subjects. *Invest Ophthalmol Vis Sci*. 2004;45:3073–3080.
14. Pons ME, Ishikawa H, Gürses-Özden R, Liebmann JM, Dou H, Ritch R. Assessment of retinal nerve fiber layer internal reflectivity in eyes with and without glaucoma using optical coherence tomography. *Arch Ophthalmol*. 2000;118:1044–1047.
15. Dwelle J, Liu S, Wang B, et al. Thickness, phase retardation, birefringence, and reflectance of the retinal nerve fiber layer in normal and glaucomatous non-human primates. *Invest Ophthalmol Vis Sci*. 2012;53:4380–4395.
16. Vermeer KA, van der Schoot J, Lemij HG, de Boer JF. RPE-normalized RNFL attenuation coefficient maps derived from volumetric OCT imaging for glaucoma assessment. *Invest Ophthalmol Vis Sci*. 2012;53:6102–6108.
17. Liu S, Wang B, Yin B, et al. Retinal nerve fiber layer reflectance for early glaucoma diagnosis. *J Glaucoma*. 2014;23:e45–e52.
18. Hood D, Kardon R. A framework for comparing structural and functional measures of glaucomatous damage. *Prog Retin Eye Res*. 2007;26:688–710.
19. Garway-Heath D, Caprioli J, Fitzke F, Hitchings R. Scaling the hill of vision: the physiological relationship between light sensitivity and ganglion cell numbers. *Invest Ophthalmol Vis Sci*. 2000;41:1774–1782.
20. Pathak M, Demirel S, Gardiner SK. Nonlinear, multilevel mixed-effects approach for modeling longitudinal standard automated perimetry data in glaucoma. *Invest Ophthalmol Vis Sci*. 2013;54:5505–5513.
21. Pathak M, Demirel S, Gardiner SK. Nonlinear trend analysis of longitudinal pointwise visual field sensitivity in suspected and early glaucoma. *Transl Vis Sci Technol*. 2015;4:8.

22. Datta S, Satten GA. A signed-rank test for clustered data. *Biometrics*. 2008;64:501–507.
23. Galbraith S, Daniel JA, Vissel BA. Study of clustered data and approaches to its analysis. *J Neuroscience*. 2010;30:10601–10608.
24. Chauhan BC, Malik R, Shuba LM, Rafuse PE, Nicolela MT, Artes PH. Rates of glaucomatous visual field change in a large clinical population. *Invest Ophthalmol Vis Sci*. 2014;55:4135–4143.
25. Townsend KA, Wollstein G, Schuman JS. Imaging of the retinal nerve fibre layer for glaucoma. *Br J Ophthalmol*. 2009;93:139–143.
26. Leung CK-S. Diagnosing glaucoma progression with optical coherence tomography. *Curr Opin Ophthalmol*. 2014;25:104–111.
27. Miki A, Medeiros FA, Weinreb RN, et al. Rates of retinal nerve fiber layer thinning in glaucoma suspect eyes. *Ophthalmology*. 2014;121:1350–1358.
28. Mwanza J-C, Chang RT, Budenz DL, et al. Reproducibility of peripapillary retinal nerve fiber layer thickness and optic nerve head parameters measured with Cirrus HD-OCT in glaucomatous eyes. *Invest Ophthalmol Vis Sci*. 2010;51:5724–5730.
29. Gao W, Jonnal RS, Cense B, Kocaoglu OP, Wang Q, Miller DT. Measuring directionality of the retinal reflection with a Shack-Hartmann wavefront sensor. *Optics Exp*. 2009;17:23085–23097.
30. Nouri-Mahdavi K, Brigatti L, Weitzman M, Caprioli J. Comparison of methods to detect visual field progression in glaucoma. *Ophthalmology*. 1997;104:1228–1236.

Investigative Ophthalmology & Visual Science